UNIVERSITY OF BIRMINGHAM
University of Birmingham Research at Birmingham

Threshold photoelectron–photoion coincidence spectroscopy study of CHCl2F+, CHClF+2 and CH2ClF+: Steric influence of the chlorine, fluorine and hydrogen atoms

Howle, Christopher; Collins, DJ; Tuckett, Richard; Malins, AER

DOI:
10.1039/b501838b

Citation for published version (Harvard):
Howle, C, Collins, DJ, Tuckett, R & Malins, AER 2005, 'Threshold photoelectron–photoion coincidence spectroscopy study of CHCl2F+, CHClF+2 and CH2ClF+: Steric influence of the chlorine, fluorine and hydrogen atoms', *Physical Chemistry Chemical Physics*, vol. 7, no. 11, pp. 2287-2297. https://doi.org/10.1039/b501838b

Link to publication on Research at Birmingham portal

General rights
Unless a licence is specified above, all rights (including copyright and moral rights) in this document are retained by the authors and/or the copyright holders. The express permission of the copyright holder must be obtained for any use of this material other than for purposes permitted by law.

•Users may freely distribute the URL that is used to identify this publication.
•Users may download and/or print one copy of the publication from the University of Birmingham research portal for the purpose of private study or non-commercial research.
•User may use extracts from the document in line with the concept of 'fair dealing' under the Copyright, Designs and Patents Act 1988 (?)
•Users may not further distribute the material nor use it for the purposes of commercial gain.

Where a licence is displayed above, please note the terms and conditions of the licence govern your use of this document.

When citing, please reference the published version.

Take down policy
While the University of Birmingham exercises care and attention in making items available there are rare occasions when an item has been uploaded in error or has been deemed to be commercially or otherwise sensitive.

If you believe that this is the case for this document, please contact UBIRA@lists.bham.ac.uk providing details and we will remove access to the work immediately and investigate.

Download date: 05. May. 2023

RESEARCH PAPER

PCCP
www.rsc.org/pccp

Threshold photoelectron–photoion coincidence spectroscopy study of $CHCl_2F^+$, $CHClF_2^+$ and CH_2ClF^+: Steric influence of the chlorine, fluorine and hydrogen atoms†

Chris R. Howle,‡[a] Daniel J. Collins,[b] Richard P. Tuckett*[a] and Andrew E. R. Malins[c]

[a] *School of Chemistry, University of Birmingham, Edgbaston, Birmingham, UK B15 2TT. E-mail: r.p.tuckett@bham.ac.uk; Fax: +44 121 414 4403; Tel: +44 121 414 4425*
[b] *Department of Physics, Reading University, Reading, UK RG6 2AF*
[c] *CCLRC Daresbury Laboratory, Daresbury, Warrington, UK WA4 4AD*

Received 4th February 2005, Accepted 18th April 2005
First published as an Advance Article on the web 10th May 2005

The threshold photoelectron spectrum and threshold photoelectron–photoion coincidence spectra of $CHCl_2F$, $CHClF_2$ and CH_2ClF are reported in the range 11.3–24.8 eV. Tunable photoionizing radiation with a resolution of 0.3 nm is provided from a synchrotron source with a vacuum-UV monochromator. The coincidence spectra are recorded continuously as a function of photon energy, allowing yields of the fragment ions to be obtained. Energetic comparisons suggest that the major products of the titled molecules dissociate in a similar manner at low photon energy, with the parent and first fragment ion, corresponding to cleavage of the weakest bond, appearing at their thermochemical thresholds. The second major ion, corresponding to cleavage of the second weakest bond, is formed *ca.* 1 eV higher than its predicted threshold, this disparity implying state-selected dissociation. $CHCl_2F$ and $CHClF_2$ fragment in a similar manner at higher photon energies, with minor ions formed by the cleavage of three bonds possessing lower appearance energies than fragment ions formed by the cleavage of two bonds. CH_2ClF displays the more expected behaviour, namely sequential bond cleavage as the photon energy increases. These observations can be rationalised in terms of the height of the barrier on the exit channel, as determined by the steric bulk of the leaving group. For the three titled molecules, mean translational kinetic energy releases have also been measured into the channels involving C–F or C–Cl bond fission. These data infer that impulsive dissociations occur at lower energy, with a trend towards statistical behaviour with increasing photon energy. Competition between statistical and impulsive processes is observed, for example C–Cl *vs.* C–F bond cleavage in $CHCl_2F^+$ and $CHClF_2^+$.

1. Introduction

The search for replacements to the chlorofluorocarbons (CFCs) has been conducted at pace since it was first postulated that chlorine atoms, once liberated from the CFC precursor, could initiate the depletion of stratospheric ozone.[1] Although it would seem easier to avoid their use completely, CFCs exhibit properties that convey substantial advantages to certain applications, such as the use of CCl_2F_2 as a commercial refrigerant. Therefore, the utilisation of hydrochlorofluorocarbons (HCFCs) as interim replacements for the CFCs has been widely accepted. Molecules in this class all contain one or more hydrogen atoms, which are susceptible to attack by the OH radical in the troposphere, thus they do not reach the upper atmosphere in significant abundance.[2] However, they possess the possibility for ozone attack if they do arrive at the stratosphere, as they still contain chlorine atoms. It is apparent that a clear understanding of the removal processes of these molecules from the atmosphere is of worldwide importance. For this reason we present a study of the vacuum-UV (VUV) fragmentation of the valence states of the HCFC parent ions $CHCl_2F^+$, $CHClF_2^+$ and CH_2ClF^+.

$CHClF_2$ has been used as an alternative for CCl_2F_2, the ozone depleting potential of the former being 20 times smaller.[2] This HCFC has been the subject of electron impact mass spectrometry, both with thermal and molecular beam sources (these two experiments being given the acronyms EIMS and MBEIMS),[3,4] and VUV photoionization mass spectrometry (PIMS).[5,6] Only the EIMS technique using a thermal source has been used to study $CHCl_2F$, although the onset of ionization has been measured by PIMS.[3,6] Both of these HCFCs have been used in the semiconductor dry etching industry.[7] By contrast, there is currently a dearth of experimental data on CH_2ClF. All three molecules have been investigated using non-threshold He(I) and He(II) photoelectron spectroscopy [8,9] and by recent *ab initio* molecular orbital calculations.[10,11] In this study we present an extension to previous work on these three HCFCs by recording the threshold photoelectron spectrum (TPES) and threshold photoelectron–photoion coincidence spectrum (TPEPICO) for each molecule, using synchrotron radiation as the tunable VUV photon source. These data allow the state-selected fragmentation of each parent ion to be studied from the onset of ionization, *ca.* 12 eV, up to 25 eV. Breakdown diagrams, which display the probability of formation for each fragment ion as a function of photon energy, are subsequently produced for comparison with results of the reactions between each HCFC and a variety of small gas-phase cations.[12] The analysis of TPEPICO experiments performed at high time resolution yields the mean translational kinetic energy release for unimolecular fragmentation processes. The results can be compared to model predictions in order to reveal the allocation of excess energy in the ionic products and the mechanism of dissociation.

† Electronic supplementary information (ESI) available: Colour versions of Figs. 1–6. See http://www.rsc.org/suppdata/cp/b5/b501838b/
‡ Present address: School of Chemistry, University of Bristol, Cantock's Close, Bristol, UK BS8 1TS.

DOI: 10.1039/b501838b

2. Experimental

The apparatus for performing TPEPICO experiments has been described in detail elsewhere.[13,14] The experiments were performed at station 3.2 of the Daresbury Synchrotron Radiation Source, which is equipped with a 5 m McPherson normal-incidence monochromator.[15] The monochromatised synchrotron radiation is coupled into a capillary of 2 mm id and reaches the interaction region, where the gaseous sample is admitted. The photon flux is monitored using a photomultiplier tube, in conjunction with the visible fluorescence from a sodium salicylate coated Pyrex window, allowing flux normalisation of the data. The threshold electron analyser consists of a cylindrical electrostatic lens followed by a 127° post analyser, which rejects energetic electrons. The lens has a very shallow depth of field and very poor chromatic aberrations, so that only electrons with low initial energies produced in the centre of the interaction region focus efficiently at the entrance of the post analyser. Simulations suggest a high degree of space focusing, so that a finite interaction volume is relatively unimportant.[13] The resolution of the electron analyser, *ca.* 10 meV, is superior to that used in the monochromator, 0.3 nm in our experiments. This latter resolution corresponds to 35 meV at 12 eV and 150 meV at 25 eV. Therefore, the resolution of the experiment is limited by that of the photon source. Ions pass through a two-stage acceleration region, followed by a linear time-of-flight (TOF) drift tube. This arrangement also satisfies the space focusing condition,[16] which yields sufficient TOF resolution that kinetic energy releases from dissociative ionization processes can be measured with no significant degradation of the collection efficiency. A 20 V cm^{-1} DC electric extraction field withdraws both electrons and ions from the interaction region, whereupon they are detected by a channeltron (Phillips X818BL) and a pair of microchannel plates (Hamamatsu F4296-10), respectively. Raw signals from both detectors are discriminated and conveyed to a time-to-digital converter (TDC) card *via* pulse-shaping electronics. The electron signal provides the start pulse, with the ion signal providing the stop pulse, thus delayed coincidences can be recorded. A counter card, working in parallel with the TDC card, facilitates the concurrent measurement of total ion and threshold photoelectron spectra.

Using this apparatus three kinds of experiments can be performed. First, a TPES of either $CHCl_2F$, $CHClF_2$ or CH_2ClF is recorded by measuring the threshold photoelectron signal as a function of excitation energy. The monochromator was calibrated by recording the peaks in the TPES of Ar at 15.759 and 15.937 eV, corresponding to ionization to the $^2P_{3/2}$ and $^2P_{1/2}$ states of Ar^+, respectively.[17] Second, a TPEPICO spectrum, in the form of a 3-D histogram of ion TOF *vs.* coincidence counts *vs.* photon energy of the relevant molecule is collected. The TOF resolution is limited by a desire to observe all possible ion fragments over 256 channels, yet maintain sufficient wavelength channels in the spectrum. This limitation results in a small degree of uncertainty in the identification of ion fragments with similar masses, and hence similar TOFs. As the TOF is approximately proportional to $(mass)^{1/2}$, this problem is at its most acute in instances involving possible hydrogen-atom loss, such as the $CCl^+/CHCl^+$ and CF^+/CHF^+ ionic fragments, which have predicted TOFs of 12.01/12.13 and 9.70/9.86 μs, respectively. These values infer differences of only *ca.* two or three TOF channels when using the TOF resolution employed in this work of 64 ns. The presence of $^{35}Cl/^{37}Cl$ isotope effects in the former case complicates the assignment issue further. As a result, each pair of ions with small mass difference will be considered together, giving composite ion yield plots. From the TPEPICO histogram, a cut at fixed TOF gives yields for each fragment ion observed, with background subtraction removing false coincidences. Subsequently, a breakdown diagram can be composed, showing relative ion abundance *vs.* photon energy, for each molecule; these data were published and compared with product branching ratios from a recent ion–molecule study by us.[12] Third, high-resolution (8 ns) fixed-energy TPEPICO spectra can be obtained, yielding 2-D data of coincidence counts *vs.* ion TOF. This resolution is the optimum that can be used with the current TDC card. Analysis of these peak shapes gives the kinetic energy release distribution and hence the mean translational kinetic energy release, $\langle KE \rangle_t$, for each ion fragment that results from a single bond cleavage of the parent ion.[18,19] The fitting procedure allows for the various isotopomers of the three molecules studied,[20] with the peaks for fragment ions containing one or more Cl atoms necessarily being asymmetric to long time of flight. Each $\langle KE \rangle_t$ value can be divided by the available energy, E_{avail}, to give the fraction of energy that is channelled into the translational motion of the fragments, $\langle f \rangle_t$. E_{avail} is equal to the excitation photon energy plus the thermal energy of the parent molecule at 298 K minus the appropriate thermochemical threshold for forming the daughter ion. For cleavage of the weakest bond (*e.g.* formation of $CHClF^+ + Cl$ from $(CHCl_2F^+)^*$), the appearance energy at 298 K (AE_{298}) is used since these species turn on at the thermochemical threshold (Section 4). For cleavage of the second-weakest bond (*e.g.* formation of $CHCl_2^+ + F$ from $(CHCl_2F^+)^*$), since the fragment ions always turn on at least 1 eV above the thermochemical threshold (Section 4) it is now not appropriate to use AE_{298}. Instead, we use the calculated enthalpy change for the reaction ($\Delta_r H^0_{298,calc}$—see Section 3), giving a predicted appearance energy at 298 K for the fragment ion following the Traeger and McLoughlin correction described in Section 3.[21] The thermal energies of $CHCl_2F$, $CHClF_2$ and CH_2ClF at 298 K were calculated as 0.073, 0.064 and 0.052 eV, respectively. Each of these values comprises a rotational and vibrational contribution, with the vibrational frequencies taken from standard literature sources.[22]

A comparison of the experimental values of $\langle f \rangle_t$ with those determined by both statistical and impulsive models indicates the method of dissociation of the parent ion at a particular photon energy. A statistical dissociation proceeds *via* a parent ion photoexcited to an electronic state that has a sufficiently long lifetime that energy randomisation is permitted prior to dissociation. Internal conversion can occur to the electronic ground state, and dissociation proceeds from that potential energy surface, resulting in a relatively low fractional KE release. A lower limit to the statistical $\langle f \rangle_t$ can be estimated using $1/(x + 1)$, where x is the number of vibrational degrees of freedom in the transition state of the unimolecular dissociation.[23] x takes the value $3N - 7$, where N is the number of atoms in the parent molecule. As each of the molecules in this study has five atoms, we calculate a lower limit of $\langle f \rangle_t$ for $CHCl_2F$, $CHClF_2$ and CH_2ClF of 0.11. Impulsive dissociations are characterised by a short-lived excited precursor that fragments on a timescale comparable to, or faster than, that of processes such as internal molecular motion, intramolecular vibrational redistribution or electronic relaxation. One model for this type of dissociation assumes the two atoms of the cleaved bond recoil with a force large enough to allow intramolecular collisions between the excited atom and the other recoiling fragment. This leads to substantial vibrational energy transfer into the fragments. For this model, $\langle f \rangle_t$ can be estimated classically by the simple kinematic relation[24]

$$\langle f \rangle_t = \frac{\langle KE \rangle_t}{E_{avail}} = \frac{\mu_b}{\mu_f} \qquad \text{(I)}$$

where μ_b is the reduced mass of the two atoms whose bond is broken and μ_f is the reduced mass of the two product fragments formed by the dissociation. Therefore, such dissociations resulting from single bond fission will have different $\langle f \rangle_t$ values depending on the bond that is cleaved and the precursor

 This journal is © The Owner Societies 2005

Table 1 Energetics of the ionization pathways of $CHCl_2F$, $CHClF_2$ and CH_2ClF

	AE_{298}[d]/eV	$\Delta_r H^0_{298,exp}$[e]/eV	$\Delta_r H^0_{298,calc}$[f]/eV
Major[a] ion products of $CHCl_2F$ (−283)[c]			
$CHCl_2F^+$ (+829) + e^-	11.50 (5)		11.53
$CHClF^+$ (+743) + Cl (+121) + e^-	11.73 (5)	11.85 (5)	11.89
$CHCl_2^+$ (+887) + F (+79) + e^-	14.4 (2)	14.52 (20)	12.95
Minor[b] ion products of $CHCl_2F$ (−283)			
CF^+(+1134) + HCl(−92) + Cl(+121) + e^-	15.5 (1)		14.99
+ Cl_2(0) + H(+218) + e^-			16.95
+ 2Cl(+142) + H(+218) + e^-			19.46
CHF^+(+1121) + Cl_2(0) + e^-	> 15.5 (1)		14.55
+ 2Cl(+142) + e^-			17.07
CCl^+(+1243) + HF(−273) + Cl(+121) + e^-	17.1 (1)		14.25
+ HCl(−92) + F(+79) + e^-			15.69
+ ClF(−50) + H(+218) + e^-			17.56
+ Cl(+121) + F(+79) + H(+218) + e^-			20.16
$CHCl^+$(+1247) + ClF(−50) + e^-	> 17.1 (1)		15.34
+ Cl(+121) + F(+79) + e^-			17.94
Major[a] ion products of $CHClF_2$ (−482)			
$CHClF_2^+$ (+694) + e^-	12.15 (5)		12.18
CHF_2^+ (+604) + Cl (+121) + e^-	12.25 (5)	12.36 (5)	12.51
$CHClF^+$ (+743) + F (+79) + e^-	14.3 (1)	14.42 (10)	13.52
Minor[b] ion products of $CHClF_2$ (−482)			
CF_2^+(+922) + HCl(−92) + e^-	14.3 (4)		13.59
+ Cl(+121) + H(+218) + e^-			18.06
CF^+(+1134) + HF(−273) + Cl(+121) + e^-	16.0 (2)		15.18
+ HCl(−92) + F(+79) + e^-			16.61
+ ClF(−50) + H(+218) + e^-			18.48
+ Cl(+121) + F(+79) + H(+218) + e^-			21.08
CHF^+(+1121) + ClF(−50) + e^-	> 16.0 (2)		16.09
+ Cl(+121) + F(+79) + e^-			18.69
Major[a] ion products of CH_2ClF (−262)			
CH_2ClF^+ (+869) + e^-	11.63 (5)		11.72
CH_2F^+ (+833) + Cl (+121) + e^-	12.57 (5)	12.67 (5)	12.61
CH_2Cl^+ (+959) + F (+79) + e^-	14.1 (1)	14.20 (10)	13.38
Minor[b] ion products of CH_2ClF (−262)			
CHF^+(+1121) + HCl(−92) + e^-	13.4 (2)		13.38
+ Cl(+121) + H(+218) + e^-			17.85
CH_2^+(+1386) + ClF(−50) + e^-	16.6 (5)		16.56
+ Cl(+121) + F(+79) + e^-			19.16
$CHCl^+$(+1247) + HF(−273) + e^-	16.8 (2)		12.81
+ F(+79) + H(+218) + e^-			18.72
CCl^+(+1243) + HF(−273) + H(+218) + e^-	17.4 (1)		15.03
+ H_2(0) + F(+79) + e^-			16.42
+ 2H(+436) + F(+79) + e^-			20.94

Table 1 (*continued*)

$CF^+(+1134) + H_2(0) + Cl(+121) + e^-$	21.8 (2)	15.72
$+ HCl(-92) + H(+218) + e^-$		15.77
$+ 2H(+436) + Cl(+121) + e^-$		20.24

[a] Major ion product is defined as either the parent ion, or a fragment ion caused by fission of a single bond. [b] Minor ion product is defined as a fragment ion caused by fission of multiple bonds. [c] Literature values for $\Delta_f H^o_{298}$, given in brackets in Column 1, have units of kJ mol^{-1} (see Section 3). [d] Experimentally determined appearance energies, taken as the first onset of ion signal above the noise. Errors in the lowest decimal place are given in brackets. [e] The value of $\Delta_r H^o_{298,exp}$ is derived from AE_{298} of the fragment ion using the procedure of Traeger and McLoughlin.[21] Errors in the lowest decimal place are given in brackets. [f] The value of $\Delta_r H^o_{298,calc}$ is given by the enthalpy of formation of products minus that of reactants; we use values for $\Delta_f H^o_{298}$ given in brackets in Column 1, where the units are kJ mol^{-1}.

molecule. We should note that, in this simple description of impulsive dissociation, there is no differentiation between soft and hard models,[19] where the former and latter are sometimes described as the pure and modified models, respectively.[25]

3. Energetics of the ionic dissociation channels of $CHCl_2F$, $CHClF_2$ and CH_2ClF

The energetics of the important ionic dissociation channels resulting from photodissociation of $CHCl_2F$, $CHClF_2$ and CH_2ClF are given in Table 1. The AE_{298} values measured in this work are listed in column 2, these values being determined from the first observation of signal above the background noise for each fragment ion. For the *major* fragment ions, defined as those products formed by single bond cleavage, AE_{298} is converted into an upper limit of $\Delta_r H^0_{298}$ for the appropriate unimolecular reaction using the procedure of Traeger and McLoughlin,[21] and is given in column 3 (denoted as $\Delta_r H^0_{298,exp}$). This procedure is discussed in more detail in our previous work.[26] The vibrational frequencies of the fragment ions were not available in their entirety. In these instances, values for $BHCl_2$, BHF_2 and CH_2O, isoelectronic with $CHCl_2^+$, CHF_2^+ and CH_2F^+, were used.[22] The predicted enthalpies of reaction at 298 K ($\Delta_r H^0_{298,calc}$) listed in column 4 are the sum of the enthalpies of formation of the products minus that of the neutral reactant, using the bracketed values given in units of kJ mol^{-1} in column 1. These enthalpies of formation at 298 K are taken from standard reference sources,[22,27] apart from those of CHF_2^+ [26] and CF_2^+, which is calculated as the enthalpy of formation of CF_2 plus the ionization energy of CF_2. A loose comparison of the AE_{298} for each minor ion with the $\Delta_r H^0_{298,calc}$ values allows the neutral partner(s) that form with each fragment ion to be elucidated.

4. Results

4.1 $CHCl_2F$

4.1.1 Threshold photoelectron spectrum. The TPES of $CHCl_2F$ was recorded from 11.3 to 24.8 eV at an optical resolution of 0.3 nm (Fig. 1a). The onset of ionization is 11.50 ± 0.05 eV. This value is significantly lower than that obtained by PIMS, 11.75 ± 0.02 eV,[6] and must cast some doubt on the accuracy of this earlier study. Peaks occurring at 11.99, 12.10, 12.41, 13.02, 14.54, 14.74, 17.77, 18.72 and 21.82 eV correspond to the vertical ionization energies (VIEs) of the $\tilde{X}\ ^2A''$, $\tilde{A}\ ^2A'$, $\tilde{B}\ ^2A''$, $\tilde{C}\ ^2A'$, $\tilde{D}\ ^2A''$, $\tilde{E}\ ^2A'$, $\tilde{F}\ ^2A'/\tilde{G}\ ^2A''$, $\tilde{H}\ ^2A'$ and $\tilde{I}\ ^2A'$ states. The ground and first excited states appear as shoulders on the $\tilde{B}\ ^2A''$ state peak, and are assigned in accordance with previous photoelectron spectra recorded at higher resolution.[9] These VIE values are in excellent agreement with He(I) and He(II) photoelectron spectra[8,9] and, to a lesser extent, calculations of molecular orbital binding energies using *ab initio* methods.[10] The first four bands correspond to ionization from chlorine 3pπ lone pair orbitals, with the fifth band (ionization to $\tilde{D}\ ^2A''$) corresponding to removal of a C–Cl σ-bonding electron. These five orbitals possess 99, 87, 98, 93 and 60% Cl 3p character, respectively.[10] The $\tilde{E}\ ^2A'$ state is essentially fluorine nonbonding in character, whilst the unresolved $\tilde{F}\ ^2A'/\tilde{G}\ ^2A''$ states are C–Cl bonding and F nonbonding in nature. The $\tilde{H}\ ^2A'$ and $\tilde{I}\ ^2A'$ states pertain to a blend of C–H and C–F σ-bonding orbitals and the C 2s nonbonding orbital, respectively.[9]

4.1.2 Scanning-energy TPEPICO spectra. The scanning-energy TPEPICO spectrum of $CHCl_2F$ was measured from 11.3 to 24.8 eV at a photon resolution of 0.3 nm and an ion TOF resolution of 64 ns. The intrinsic limitations when using this TOF resolution were discussed in Section 2, and lead to detection of five ionic species from the colour map; $CHCl_2F^+$, $CHClF^+$, $CHCl_2^+$, CF^+/CHF^+ and $CCl^+/CHCl^+$. Ion yields for these products are constructed as detailed earlier and are

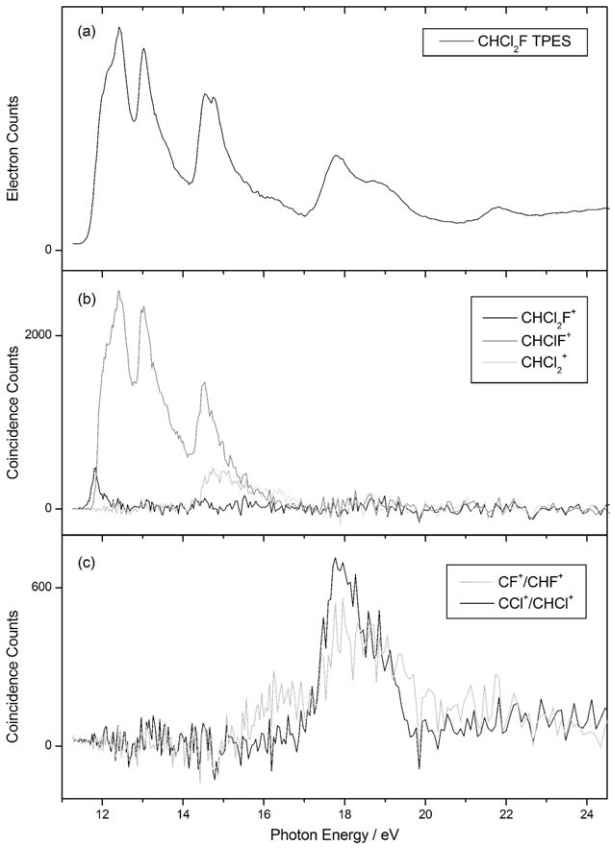

Fig. 1 (a) Threshold photoelectron spectrum of $CHCl_2F$. (b), (c) TPEPICO coincidence ion yields of $CHCl_2F^+$, $CHClF^+$, $CHCl_2^+$, CF^+/CHF^+ and $CCl^+/CHCl^+$. In all cases, the resolution is 0.3 nm.

 This journal is © The Owner Societies 2005

Table 2 Comparison of appearance energies (AE_{298}) of the various fragment ions of $CHCl_2F$ and $CHClF_2$ with previous experimental data. Errors are given in parentheses

	AE_{298}[c]/eV	PIMS[d]/eV	EIMS[e]/eV	MBEIMS[f]/eV
Major[a] ion products of $CHCl_2F$				
$CHCl_2F^+$	11.50 (5)	11.75 (2)[g]	12.39 (20)	
$CHClF^+$	11.73 (5)		12.69 (15)	
$CHCl_2^+$	14.4 (2)			
Minor[b] ion products of $CHCl_2F$				
CF^+	15.5 (1)		16.9 (2)	
CHF^+	>15.5 (1)			
CCl^+	17.1 (1)		18.3 (2)	
$CHCl^+$	>17.1 (1)		19.0 (2)	
Major[a] ion products of $CHClF_2$				
$CHClF_2^+$	12.15 (5)	12.16 (2)[h]	12.69 (15)	12.50 (5)
CHF_2^+	12.25 (5)	12.39[h]	12.59 (15)	12.24 (3)
$CHClF^+$	14.3 (1)	14.28[h]	15.11 (15)	14.79 (10)
Minor[b] ion products of $CHClF_2$				
CF_2^+	14.3 (4)	18.79[h]	16.1 (3)	15.36 (10)
CF^+	16.0 (2)	15.90[h]	17.30 (15)	15.8 (1)
CHF^+	>16.0 (2)	18.50[h]		

[a] Major ion product is defined as either the parent ion, or a fragment ion caused by fission of a single bond. [b] Minor ion product is defined as a fragment ion caused by fission of multiple bonds. [c] Experimentally determined appearance energies, taken as the first onset of ion signal above the noise. [d] Appearance energies determined using photoionization mass spectrometry (PIMS).[5,6] [e] Appearance energies determined using electron impact mass spectrometry (EIMS).[3] [f] Appearance energies determined using crossed electron/molecular beam electron impact mass spectrometry (MBEIMS).[4] [g] Ref. 6. [h] Ref. 5.

shown in Fig. 1b and 1c. The parent ion yield is of extremely low intensity and is only observed up to 12.2 eV, with a maximum at 11.8 eV. There is no evidence for loss of a hydrogen atom from the parent ion over this limited span of energies. The appearance energy of $CHClF^+$ is 11.73 ± 0.05 eV, which can be compared with the 0 K value of 11.92 ± 0.01 eV measured using a different TPEPICO apparatus.[28] We note that this latter experiment used a much higher resolution TOF analyser, and the quality of the data allowed for a full fit of the threshold region to extract 0 K thresholds. This procedure is not justified for our experiment, but our threshold at 298 K is lower than that extracted at 0 K by Sztaray and Baer,[28] as expected. By contrast, agreement is poor when either value is compared to the EIMS value of 12.69 ± 0.15 eV.[3] This difference can be explained by the gradual threshold law for ionization by electrons.[29] Another reason for the difference is the inherent lack of resolution in most electron impact apparatus from that era, typically *ca.* 0.3 eV.[30] These limitations can therefore account for the anomalies observed between the AE_{298} values obtained in this work and those by the EIMS technique (see columns 2 and 4 in Table 2). $CHClF^+$ is the major fragment ion resulting from photodissociation from the $\tilde{X}\ ^2A''$, $\tilde{A}\ ^2A'$, $\tilde{B}\ ^2A''$and $\tilde{C}\ ^2A'$ states of the parent cation. From its appearance energy at 14.4 ± 0.2 eV, $CHCl_2^+$ provides competition for dissociation with the $CHClF^+$ channel from the $\tilde{D}\ ^2A''$ and $\tilde{E}\ ^2A'$ states. The intensity of this ion signal is significantly less than that of $CHClF^+$, and we note that it was not observed in the EIMS study.

Multiple bond cleavages can occur at higher photon energies. CF^+/CHF^+ signal is first observed at 15.5 ± 0.1 eV. Careful consideration of the peak shape and centre in the TOF mass spectrum (TOF-MS) leads us to conclude that this signal is purely due to CF^+ at onset. However, this signal is considered to be a mixture of the two ions at higher photon energies. $CCl^+/CHCl^+$ is seen at an appearance energy of 17.1 ± 0.1 eV, which is unambiguously determined to be from CCl^+ production at this energy. A blend of both CCl^+ and $CHCl^+$ signals is observed at higher photon energies. These assignments are supported by the results of ion–molecule reactions reported recently,[12] where the resolution of the detection quadrupole mass spectrometer used in that study is superior to that of the linear TOF analyser used here. This ordering of fragments is also observed in the EIMS study, as CCl^+ is detected at 18.3 ± 0.2 eV, 0.7 eV lower in energy than the appearance energy of $CHCl^+$ (Table 2). Both CF^+/CHF^+ and $CCl^+/CHCl^+$ are the only product ions formed by dissociation from the $\tilde{F}\ ^2A'/\tilde{G}\ ^2A''$ and $\tilde{H}\ ^2A'$ states of the parent ion. HCl or HF elimination, and the observation of $CClF^+$ or CCl_2^+ is not observed in this study, although we note that these fragment ions would appear on the shoulders to low TOF of the $CHClF^+$ and $CHCl_2^+$ peaks and might, therefore, be difficult to resolve.

4.1.3 Fixed-energy TPEPICO spectra. Fixed-energy spectra were recorded at the optimum TOF resolution of 8 ns for the $CHClF^+$ fragment ion at photon energies of 12.41, 13.02 and 14.67 eV, respectively, and for $CHCl_2^+$ at 14.67 eV. These values correspond to the Franck–Condon maxima of the $\tilde{B}\ ^2A''$, $\tilde{C}\ ^2A'$ and midway between the maxima of the $\tilde{D}\ ^2A''$ and $\tilde{E}\ ^2A'$ states of the parent ion. Mean translational kinetic energy releases, $\langle KE \rangle_t$, were obtained for each of these spectra, as described elsewhere.[18,20] Fig. 2a shows the coincidence TOF spectrum for $CHClF^+$ resulting from photodissociation of $CHCl_2F$ at 13.02 eV. A small basis set comprising four contributions ($n = 1$–4) forms the best fit and yields a $\langle KE \rangle_t$ value of 0.49 ± 0.03 eV. The reduced probability, shown in Fig. 2b, is defined as the probability of a given energy release divided by the range of energies.[20] Experimentally-determined values of

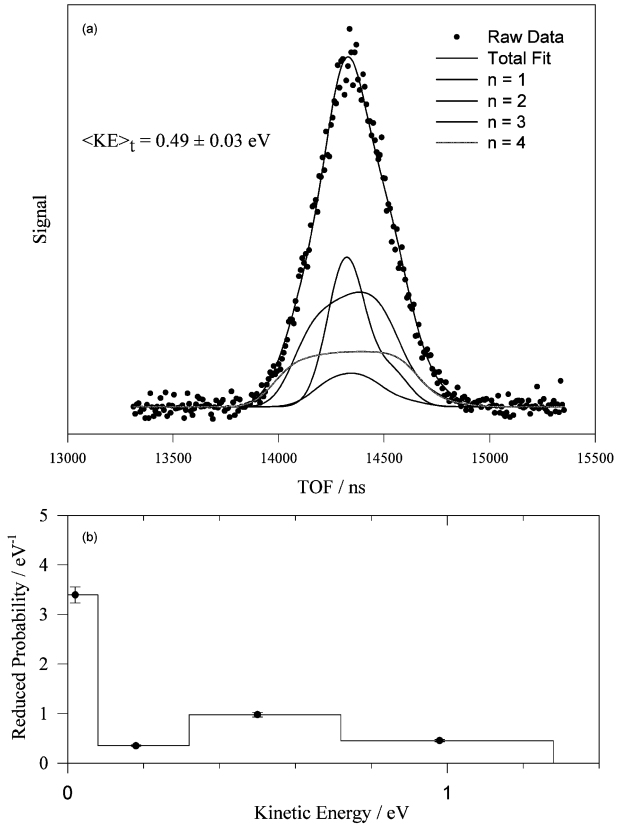

Fig. 2 Coincidence TOF spectrum (dots) of $CHClF^+$ resulting from photoionization of $CHCl_2F^+$ at 13.02 eV. The solid line gives the best fit to the data, comprised of four contributions ($n = 1$–4) in the basis set for ε_t.[19,20] The reduced probability of each contribution is shown in (b). The fit yields a total mean translational kinetic energy, $\langle KE \rangle_t$, into $CHClF^+ + Cl$ of 0.49 ± 0.03 eV, which constitutes 36% of the available energy.

$\langle KE \rangle_t$ and $\langle f \rangle_t$, together with $\langle f \rangle_t$ values calculated using statistical and pure (or soft) impulsive models, are shown in Table 3. For dissociation to $CHClF^+ + Cl$, from this limited set of data we observe that $\langle f \rangle_t$ decreases with increasing photon energy; in other words, the increase of $\langle KE \rangle_t$ is not as rapid as that of $h\nu$. The data therefore show a trend from impulsive to statistical behaviour as $h\nu$ increases, a phenomenon that has been observed previously by us in studies of similar-sized cations for cleavage of the weakest bond.[19] The single, high value of $\langle f \rangle_t$ determined for dissociation of the second weakest bond, $(CHCl_2F^+)^* \rightarrow CHCl_2^+ + F$, is assigned as being impulsive in nature. This spectrum was recorded at a photon energy only 0.27 eV above the AE_{298} of this ion. However, since this threshold and its corresponding $\Delta_r H^0_{298,exp}$ is significantly greater than the calculated $\Delta_r H^0_{298,calc}$, state-selected impulsive dissociation is probably occurring. Our high value of $\langle f \rangle_t$ confirms this conclusion.

4.2 $CHClF_2$

4.2.1 Threshold photoelectron spectrum. The TPES of $CHClF_2$ was recorded between 11.8–22.6 eV at an optical resolution of 0.3 nm, and is shown in Fig. 3a. The onset of ionization to $CHClF_2^+$ is 12.15 ± 0.05 eV. This value is in reasonable agreement with an adiabatic ionization energy determined using PIMS of 12.28 ± 0.02 eV.[6] Peaks observed at 12.70, 13.96, 15.89, 18.82 and 19.89 eV correspond to the VIEs of the $\tilde{X}\ ^2A''/\tilde{A}\ ^2A'$, $\tilde{B}\ ^2A'$, $\tilde{C}\ ^2A''/\tilde{D}\ ^2A''/\tilde{E}\ ^2A'$, $\tilde{F}\ ^2A'$ and $\tilde{G}\ ^2A'/\tilde{H}\ ^2A''$ states. These values are in good agreement with those obtained from *ab initio* studies[10,11] and in excellent agreement with non-threshold photoelectron studies.[8,9] The ground and first excited states are assigned as the chlorine 3pπ lone pair orbitals, which possess 94 and 95% Cl 3p character, respectively.[10] The $\tilde{B}\ ^2A'$ state is C–Cl σ-bonding in character, whilst the unresolved $\tilde{C}\ ^2A''/\tilde{D}\ ^2A''/\tilde{E}\ ^2A'$ states correspond to three fluorine lone pair orbitals. The remaining states are assigned as C–H σ-bonding ($\tilde{F}\ ^2A'$) and as two C–F σ-bonding orbitals ($\tilde{G}\ ^2A'/\tilde{H}\ ^2A''$).[9]

4.2.2 Scanning-energy TPEPICO spectra. The scanning energy TPEPICO spectrum of $CHClF_2$ was measured from 11.8 to 22.6 eV at a photon resolution of 0.3 nm and an ion TOF resolution of 64 ns. The same inherent limitations of resolution, as described in Section 2, apply, and four main fragment ions are identified; $CHClF_2^+$, $CHClF^+$, CF_2^+/CHF_2^+ and CF^+/CHF^+. Ion yields for these products are shown in Fig. 3b. The parent ion yield is, once more, of low intensity, spanning an energy range of 12.15–12.60 eV, with a maximum at 12.37 eV. No C–H bond fission is observed over this narrow energy range. Cleavage of a C–Cl bond is the first dissociation process, with the AE_{298} of CHF_2^+ determined as 12.25 ± 0.05 eV. This is the dominant fragment ion up to *ca.* 16 eV, with the profile of the ion yield matching that of the TPES over the maxima of the $\tilde{X}\ ^2A''/\tilde{A}\ ^2A'$ and $\tilde{B}\ ^2A'$ states. We note that a two-photon absorption study on this molecule, using an ArF

Table 3 Total mean translation kinetic energy releases, $\langle KE \rangle_t$, for the two-body fragmentation of the valence states of $CHCl_2F^+$, $CHClF_2^+$ and CH_2ClF^+

Parent ion	State	Daughter ion	$h\nu$/eV	E_{avail}[a]/eV	$\langle KE \rangle_t$/eV	$\langle f \rangle_t$ experimental[b]	$\langle f \rangle_t$ statistical	$\langle f \rangle_t$ impulsive
$CHCl_2F^+$	$\tilde{X}\ ^2A''$	$CHClF^+$	12.41	0.74	0.36 (4)	0.49	0.11	0.39
	$\tilde{A}\ ^2A'$		13.02	1.37	0.49 (3)	0.36	0.11	0.39
	$\tilde{D}\ ^2A''/\tilde{E}\ ^2A'$		14.67	3.02	0.56 (3)	0.19	0.11	0.39
	$\tilde{D}\ ^2A''/\tilde{E}\ ^2A'$	$CHCl_2^+$	14.67	1.92	0.96 (4)	0.50	0.11	0.47
$CHClF_2^+$	$\tilde{X}\ ^2A''/\tilde{A}\ ^2A'$	CHF_2^+	12.70	0.49	0.27 (3)	0.55	0.11	0.43
	$\tilde{B}\ ^2A'$		13.96	1.76	0.95 (6)	0.54	0.11	0.43
	$\tilde{C}\ ^2A''/\tilde{D}\ ^2A''/\tilde{E}\ ^2A'$		15.89	3.73	0.77 (2)	0.21	0.11	0.43
	$\tilde{C}\ ^2A''/\tilde{D}\ ^2A''/\tilde{E}\ ^2A'$	$CHClF^+$	15.89	2.55	1.22 (4)	0.48	0.11	0.50
CH_2ClF^+	$\tilde{B}$	CH_2F^+	14.03	1.51	0.75 (4)	0.50	0.11	0.52
	$\tilde{C}$		14.32	1.80	0.69 (4)	0.38	0.11	0.52
	$\tilde{C}$	CH_2Cl^+	14.32	1.09	0.54 (4)	0.50	0.11	0.54
	$\tilde{E}/\tilde{F}$		17.44	4.21	0.87 (2)	0.21	0.11	0.54

[a] For cleavage of the weakest bond, $E_{avail} = h\nu$ + thermal energy of parent molecule at 298 K (0.073, 0.064 and 0.052 eV for $CHCl_2F$, $CHClF_2$ and CH_2ClF, respectively) − AE_{298}(daughter ion). For cleavage of the second-weakest bond, AE_{298}(daughter ion) is replaced by $\Delta_r H^0_{298,calc}$ (column 4 of Table 1) corrected by the Traeger and McLoughlin[21] procedure (see text in Section 2). [b] Given by $\langle KE \rangle_t / E_{avail}$.

This journal is © The Owner Societies 2005

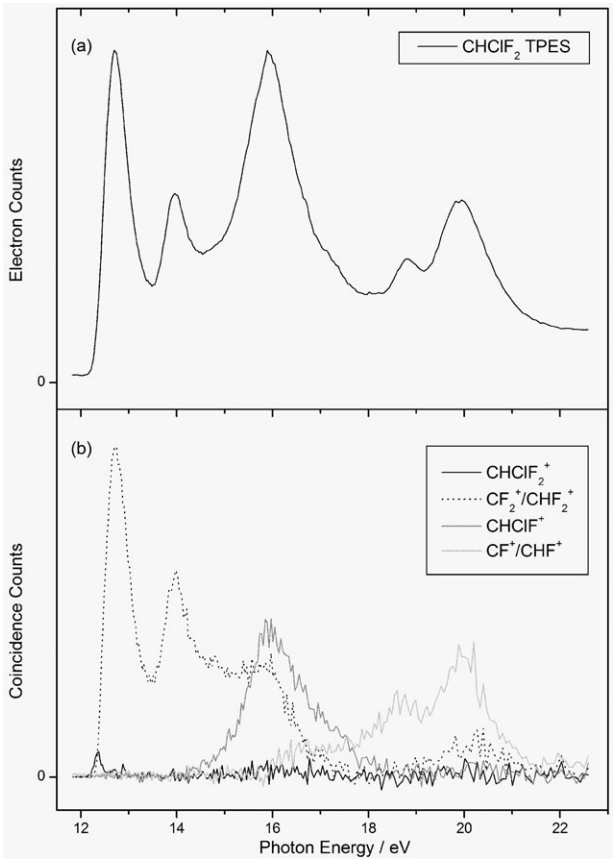

Fig. 3 (a) Threshold photoelectron spectrum of $CHClF_2$. (b) TPEPICO coincidence ion yields of $CHClF_2^+$, CF_2^+/CHF_2^+, $CHClF^+$ and CF^+/CHF^+. In all cases, the resolution is 0.3 nm.

excimer laser providing 193 nm photons, yielded CHF_2^+ as the sole ion produced.[31] Two photons of this wavelength correspond to ionization at 12.85 eV, which corroborates our observations. From close examination of the TOF-MS of this fragment, it is apparent that the signal is solely due to CHF_2^+ at low photon energies. At higher energies, however, a shift in the peak maximum to lower TOF is observed, leading us to assign a mixture of both CF_2^+ and CHF_2^+ from *ca.* 14 eV. Subsequently, the AE_{298} of CF_2^+ is determined as 14.3 ± 0.4 eV. The thermochemistry of Table 1 shows that at these energies CF_2^+ can only form with molecular HCl. The further rise in the intensity of the ion yield from *ca.* 18 eV onwards is due solely to CF_2^+, suggesting that loss of atomic Cl and H is now the dominant channel, as depicted in Table 1. The ion yield of $CHClF^+$ rises gradually from its AE_{298} of 14.3 ± 0.1 eV until it peaks at 15.85 eV, which corresponds to the maximum of the unresolved $\tilde{C}\ ^2A''/\tilde{D}\ ^2A''/\tilde{E}\ ^2A'$ states. However, significant CHF_2^+ signal is still observed at this energy, with the respective signal levels being approximately equal. This indicates there is competition between these two major, single-bond-cleavage dissociation channels from these parent ion states.

As there are several previous appearance energy measurements for fragment ions from $CHClF_2$ available in the literature,[3–5] as depicted in Table 2, a more detailed discussion of these results is warranted. Our AE_{298} values for the parent ion and first fragment ion agree reasonably well with those detected using a photon source.[5] Once more, the EIMS results do not concur with our results, due to the reasons described in Section 4.1.2. However, both of the electron impact studies report a lower appearance energy for CHF_2^+ than for the parent ion. The data given by the thermal EIMS study are only 0.1 eV apart; indeed, within the quoted errors these values are identical. The resolution of the electron beam used in the MBEIMS study is superior, 0.14 eV,[4] and it is more difficult to explain the discrepancy with our results. Although discounted by Cicman *et al.*, there is a possibility that the onset of signal in their experiment may be due to ion-pair formation, *i.e.* $CHF_2^+ + Cl^-$ are the products. Using the enthalpy of formation at 298 K for Cl^-, -227.4 kJ mol^{-1},[32] $\Delta_r H^0_{298}$ for the above reaction is 8.89 eV, making ion-pair formation energetically feasible. We note that our technique is not sensitive to formation of an ion-pair, as we record ions and electrons in coincidence that occur from the same ionization event. We suggest that the data of Cicman *et al.* may have been over-interpreted, and the apparent lower AE of CHF_2^+ compared to $CHClF_2^+$ is an artefact of the resolution of the electron beam and the deconvolution process used to determine thresholds. Our AE_{298} of $CHClF^+$ is identical to that recorded by other photoionization work and similar to that found by Cicman *et al.*; the discrepancies between our AE_{298} values and those of Hobrock *et al.*[3] have been discussed earlier. However, there is some degree of variance in the values obtained for CF_2^+, as our value, 14.3 ± 0.4 eV, lies at the lower energy end of the range of those previously reported. As CHF_2^+ is the dominant ion product from $CHClF_2$, difficulties in distinguishing between this strong signal and that of CF_2^+ have been mentioned before, possibly leading to the lack of agreement in AE values for this ion. We believe, however, that these discrepancies highlight the advantage of using photoionization over electron impact ionization to determine ionic thresholds.

A mixed signal resulting from CF^+/CHF^+ is observed as the main product from multiple bond cleavage at higher energies, with the profile mimicking that of the TPES over the $\tilde{F}\ ^2A'$ and $\tilde{G}\ ^2A'/\tilde{H}\ ^2A''$ states. Its AE_{298} is determined as 16.0 ± 0.2 eV. By closely examining the TOF-MS at the onset of signal, this value is attributed exclusively to CF^+, with CHF^+ appearing to dominate at higher photon energies. This ordering of ion fragments is in accordance with those reported by the other photon-initiated data and by our own selected ion flow tube (SIFT) experiment.[5,12] Our AE_{298} value for CF^+ is in excellent agreement with those of the PIMS and MBEIMS research, with the EIMS data proving to be anomalous again (Table 2). It should be noted that $CCl^+/CHCl^+$ ion signal is not observed in the energy range studied. These ions were also not observed by previous electron impact data [3,4] or by our SIFT study.[12] This observation is unsurprising, as the C–Cl bond is the weakest in $CHClF_2$. Therefore, fission of this bond is the primary dissociation event, as it is energetically the most favourable process.

4.2.3 Fixed-energy TPEPICO spectra. Fixed-energy spectra were recorded for the CHF_2^+ fragment ion at 12.70 and 13.96 eV, and for the CHF_2^+ and $CHClF^+$ fragments at 15.89 eV, all at a TOF resolution of 8 ns. These energies correspond to the Franck–Condon maxima of the $\tilde{X}\ ^2A''/\tilde{A}\ ^2A'$, $\tilde{B}\ ^2A'$ and $\tilde{C}\ ^2A''/\tilde{D}\ ^2A''/\tilde{E}\ ^2A'$ states of the parent ion. The experimental data for $\langle KE \rangle_t$ and $\langle f \rangle_t$, together with $\langle f \rangle_t$ values calculated using statistical and pure impulsive models, are shown in Table 3. For dissociation of $(CHClF_2^+)^*$ to $CHF_2^+ + Cl$ and cleavage of the weakest bond, we observe that $\langle f \rangle_t$ decreases as $h\nu$ increases. As with $CHCl_2F^+$ (Section 4.1.3), the data therefore suggest a trend from impulsive behaviour in the $\tilde{X}\ ^2A''/\tilde{A}\ ^2A'$ and $\tilde{B}\ ^2A'$ states of $CHClF_2^+$ to more statistical behaviour in the unresolved $\tilde{C}\ ^2A''/\tilde{D}\ ^2A''/\tilde{E}\ ^2A'$ states. The single translational release value for $CHClF^+ + F$, corresponding to cleavage of the second-weakest bond, appears to fit the impulsive model. A similar effect was observed in $CHCl_2F^+$ for fission of its C–F bond, the second weakest.

4.3 CH_2ClF

4.3.1 Threshold photoelectron spectrum. The TPES of CH_2ClF was recorded from 11.3 to 24.8 eV at an optical

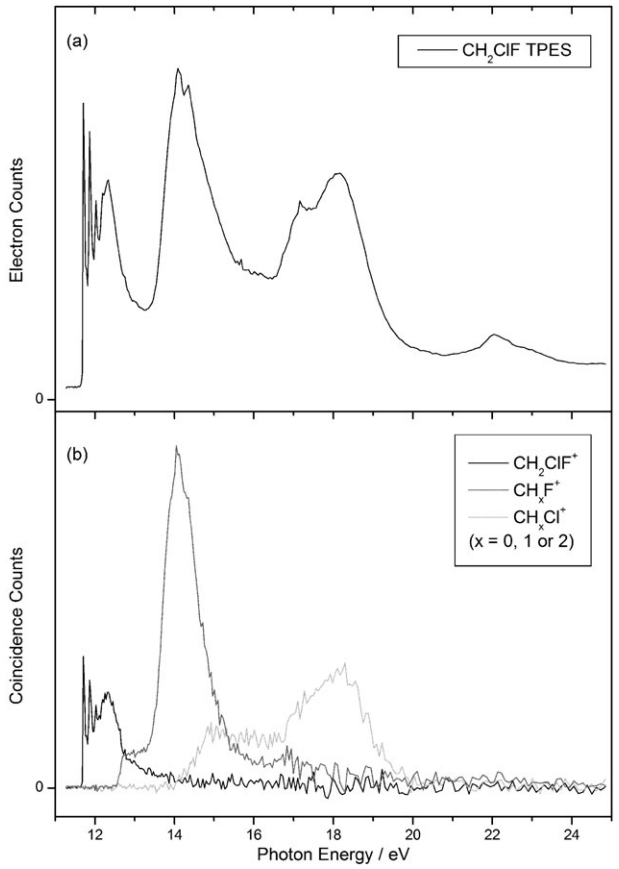

Fig. 4 (a) Threshold photoelectron spectrum of CH_2ClF. (b) TPEPICO coincidence ion yields of CH_2ClF^+, CH_xF^+ and CH_xCl^+ (where $x = 0$, 1 or 2). In all cases, the resolution is 0.3 nm.

resolution of 0.3 nm, as shown in Fig. 4a. The onset of ionization to CH_2ClF^+ is 11.63 ± 0.05 eV. Three peaks are observed with maxima occurring at 11.71, 11.87 and 12.03 eV. These are assigned as vibrational structure within the $\tilde{X}$ state, very similar to previous TPEPICO data on CH_2F_2 obtained by our group.[33] The structure in both molecules arises from excitation of the ν_2 bending mode of the CH_2 moiety, resulting primarily from the extensive decrease in the HCH bond angle upon ionization.[34] The observed spacing of 1290 cm^{-1} is in excellent agreement with *ab initio* and non-threshold photoelectron studies.[8,34] Peaks are also observed at 12.34, 14.09, 14.35, 17.16, 18.17 and 22.04 eV, corresponding to the VIEs of the $\tilde{A}$, $\tilde{B}$, $\tilde{C}$, $\tilde{D}$, $\tilde{E}/\tilde{F}$ and $\tilde{G}$ states of the parent ion. These values are in good agreement with both previous photoelectron spectra, obtained using the He(I) line as the photon source, and *ab initio* calculations.[8,10] The ground and first excited states are assigned as chlorine 3pπ nonbonding orbitals, which possess 87 and 95% Cl 3p character, respectively.[10] The $\tilde{B}$ state is a C–Cl σ-bonding orbital, whilst the next two states are both C–H σ-bonding in nature. The $\tilde{E}/\tilde{F}$ states represent a fluorine nonbonding orbital and one localised on the F atom, respectively.[8] No previous assignments for the $\tilde{G}$ state could be found in the literature. As it is observed at a similar energy and has a comparable profile to that of the $\tilde{I}$ $^2A'$ state of $CHCl_2F^+$, we provisionally assign it to have a degree of carbon 2s orbital character.

4.3.2 Scanning energy TPEPICO spectra. The scanning energy TPEPICO spectrum of CH_2ClF was measured from 11.3 to 24.8 eV at a photon resolution of 0.3 nm and an ion TOF resolution of 64 ns. With this time resolution, the ambiguity in assignment, as described in Section 2, leads to the identification of four main fragment ions; CH_2ClF^+, CH_xCl^+, CH_xF^+ and CH_2^+, where $x = 0$, 1 or 2 hydrogen atoms. Ion yields for these products are shown in Fig. 4b. The ion yield data for CH_2^+ is omitted, as the signal recorded is weak. The parent ion yield appears to match the shape of the TPES over the $\tilde{X}$ and $\tilde{A}$ states. Close inspection of the TOF-MS for hydrogen atom loss from the parent ion is inconclusive. However, Gaussian fits of high-resolution spectra at a range of photon energies suggest that there is no C–H bond fission from CH_2ClF^+ (see Section 4.3.3). The first ionic product is CH_2F^+, which is first observed at 12.57 ± 0.05 eV. This ion signal plateaus from initial ionization to *ca.* 13.4 eV, from where it increases rapidly. This value relates to a position on the TPES where the photoelectron signal is also rising rapidly towards the maximum of the $\tilde{B}$ state, whose peak value at 14.08 eV mirrors the CH_2F^+ peak maximum. This 'step' in the ion yield, alongside a simultaneous decrease in parent ion signal, suggests that the ground state and the lower vibrational levels of the first excited state are bound and non-dissociative, whilst the $\tilde{A}$ state is unbound in its higher vibrational levels. Detailed examination of the peak positions and shapes in the TOF-MS on a stepwise basis leads to the accurate determination of which product ions form as a function of photon energy. Using this method, the AE_{298} of CHF^+ is established as 13.4 ± 0.2 eV. This concurs precisely with the photon energy at which the CH_xF^+ ion yield begins to rise rapidly, with production of both CH_2F^+ and CHF^+ ions being observed up to *ca.* 17 eV. There is no further signal pertaining to any of CH_xF^+ species until the photon energy reaches 21.0 eV, which corresponds to the first rise of the $\tilde{G}$ state signal on the TPES, where exclusively CHF^+ is formed. CF^+ ions are first seen unambiguously at 21.8 ± 0.2 eV, and it is the sole ion formed at this and higher photon energies.

The appearance energy of CH_2Cl^+ is determined as 14.1 ± 0.1 eV, with the associated ion signal rising to an energy that is comparable to the maximum of the $\tilde{C}$ state, and subsequently mirroring the profile of the $\tilde{D}$ and $\tilde{E}/\tilde{F}$ states of the TPES. It appears that there is competition between C–Cl and C–F bond fission from the $\tilde{C}$ state, as there is approximately the same signal intensity for both channels at this energy. The AE_{298} of $CHCl^+$ is determined as 16.8 ± 0.2 eV using the stepwise method described above. As with CH_xF^+, this energy correlates exactly with the photon energy at which the CH_xCl^+ ion signal rises to a new, higher maximum. Thin cuts in the 3-D map, centred at TOF values of 12.26, 12.13 and 12.01 μs, with a width of only one TOF channel (64 ns) were performed; these values correspond to the TOFs of CH_2Cl^+, $CHCl^+$ and CCl^+, respectively. This procedure allows discrimination between these three fragments, but at the expense of signal/noise levels. The resulting ion yield plots allow the determination of AE_{298} for CCl^+ as 17.4 ± 0.1 eV. Prior to the onset of CCl^+ signal, we note that CH_2Cl^+ and $CHCl^+$ are the only ions detected. Once the final C–H bond is broken, however, only $CHCl^+$ and CCl^+ are observed in the TOF-MS, implying that CH_2Cl^+ formation ceases. This marked change in products is clearly illustrated in Fig. 5, where two high-resolution (8 ns) TOF spectra have been recorded at 17.29 and 18.05 eV, respectively. Quite apart from the obvious change in peak shape, the TOF value at maximum intensity shifts from 12.2 to 12.0 μs as the photon energy increases. The production of $CCl^+/CHCl^+$ continues up to *ca.* 18.8 eV, from where the former ion is detected alone. CH_2^+ ions are also observed over the energy range studied, albeit weakly, with an AE_{298} of 16.6 ± 0.5 eV being derived tentatively from close inspection of the ion yield plot.

4.3.3 Fixed-energy TPEPICO spectra. Fixed-energy spectra were recorded at the optimum TOF resolution of 8 ns for the CH_2F^+ fragment ion at 14.03 and 14.32 eV, and for the CH_2Cl^+ fragment at 14.32 and 17.44 eV. These values correspond to the Franck–Condon maxima of the $\tilde{B}$, $\tilde{C}$, and midway between the $\tilde{D}$ and $\tilde{E}/\tilde{F}$ states of the parent ion. Further spectra were recorded for the parent ion at photon energies between

 This journal is © The Owner Societies 2005

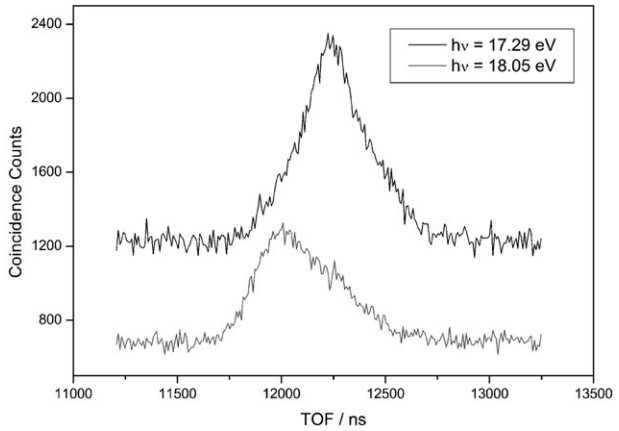

Fig. 5 High-resolution (8 ns) TOF spectrum for the CH_xCl^+ ($x = 0$, 1 or 2) fragment ion resulting from photodissociation of CH_2ClF at 17.29 and 18.05 eV.

11.7 and 12.3 eV, representing vibrationally-resolved levels of the $\tilde{X}$ state and the maximum of the $\tilde{A}$ state. A Gaussian fit, allowing for chlorine isotope effects in the parent ion, was constructed for each spectrum, with the fit to the data acquired at 11.71 eV shown in Fig. 6. There are two components, $CH_2^{35}ClF^+$ and $CH_2^{37}ClF^+$, whose heights are determined by the relative abundance of the two isotopomers, the TOF by the mass, and the full width at half maximum given by Franklin *et al.*[35] The total fit simulates the raw data excellently, displaying the 3 : 1 $^{35}Cl/^{37}Cl$ isotopic abundance. As all the other spectra also show a similar quality of fit, this indicates that there is no hydrogen loss from the parent ion at these energies.

Experimentally-determined values of $\langle KE \rangle_t$ and $\langle f \rangle_t$, together with $\langle f \rangle_t$ values calculated using statistical and impulsive models, are shown in Table 3. For dissociation of $(CH_2ClF^+)^* \rightarrow CH_2F^+ + Cl$, the limited data suggest a trend from pure impulsive behaviour in the $\tilde{B}$ state to a hybrid of the two models in the $\tilde{C}$ state. Such behaviour mirrors that of $CHCl_2F^+$ and $CHClF_2^+$ for cleavage of their weakest bond. The observation of decreasing $\langle f \rangle_t$ with increasing $h\nu$ is also noted for dissociation of the second-weakest bond, $(CH_2ClF^+)^* \rightarrow CH_2Cl^+ + F$, with the $\langle f \rangle_t$ value acquired at a photon energy of 14.32 eV, 0.50, being in good agreement with the prediction of the pure-impulsive model. The other translational release value into $CH_2Cl^+ + F$ at an energy of 17.44 eV, $\langle f \rangle_t = 0.21$, appears to lie midway between the two predicted values, and is therefore assigned as being a mixture of both dissociation models.

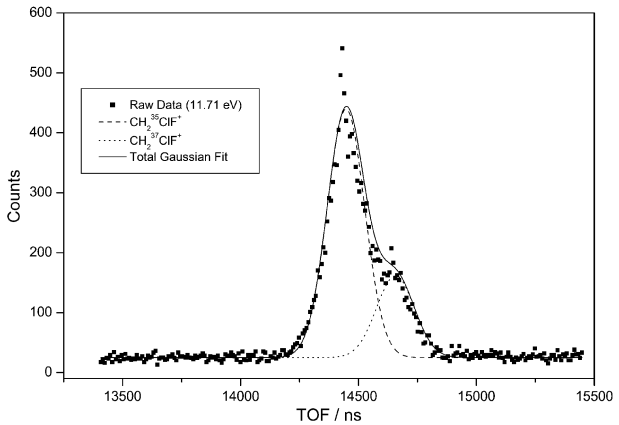

Fig. 6 High-resolution (8 ns) TOF spectrum for the CH_2ClF^+ parent ion resulting from photoionisation at 11.71 eV. The data points are fitted using a two-component Gaussian fit (one for each isotopomer of the parent ion). The DC extraction field is 20 V cm^{-1} and the temperature is 298 K.[35]

5. Discussion

5.1 Dissociation channels

The evaluation of the AE_{298} data recorded in this study and the calculated thermochemical thresholds allow the identification of the neutral fragments that accompany formation of a given fragment ion in reactions where more than one bond is cleaved. Clearly, the assignment of neutral partners in reactions where single bond fission occurs is trivial. This assessment also permits elucidation of the nature of the dissociation mechanism. Two basic models exist for dissociation dynamics, the first of which involves an absence of a barrier in the exit channel of the potential energy surface. This implies that dissociation proceeds *via* a loose transition state. Processes involving bond fission alone display these characteristics, such as $CHClF_2^+ \rightarrow CHF_2^+ + Cl$ and possibly $CHCl_2F^+ \rightarrow CF^+ + 2Cl + H$. The second category involves dissociations that have to overcome a large barrier on the exit channel, where the associated transition state is tightly constrained. Processes where bond breaking and bond making simultaneously occur fall into this group. These are of the general form $CHXClF^+ \rightarrow CHCl^+ + XF$ or $CHXClF^+ \rightarrow CF^+ + HCl + X$, where X = Cl, F or H in either case. We believe that the identity of atom X determines the height of the barrier. The larger X is, the greater the steric hindrance in the transition state, thus increasing the barrier height.[19] We refer the reader to Table 1, as extensive use of the values listed therein form the basis of this discussion.

In the case of $CHCl_2F^+$, both the parent ion and $CHClF^+$ are formed at their thermochemical thresholds as, within experimental error, the $\Delta_rH^0_{298,calc}$ values match the derived $\Delta_rH^0_{298,exp}$ values for these ions. By contrast, the $\Delta_rH^0_{298,calc}$ value for $CHCl_2^+$ production is *ca.* 1.5 eV lower than $\Delta_rH^0_{298,exp}$ for this fragment, which in turn corresponds to the maximum of the $\tilde{D}\ ^2A''$ state of the parent ion. Indeed, the ion yield signal for this fragment only occurs at energies relating to the $\tilde{D}\ ^2A''$ and $\tilde{E}\ ^2A'$ states. Therefore, this behaviour indicates state-selected dissociation. CF^+ can only be formed at the photon energy at which it is observed, 15.5 ± 0.1 eV, with HCl + Cl as the neutral partners. This process occurs *via* a tight transition state with a high barrier to reaction as X = Cl, and the AE_{298} does not match the thermochemical threshold. A possible explanation why these neutral products are preferred may be the favourable steric effect of forming a H–Cl bond, as opposed to a Cl–Cl bond, as a chlorine atom is far bulkier than a hydrogen atom. In addition, HCl + Cl formation is energetically preferred. The lowest $\Delta_rH^0_{298,calc}$ channels for CF^+ and CHF^+ predict that the larger species should be observed first. Additionally, chemical intuition suggests that the phenomenon of increasing fragmentation with increasing photon energy is to be expected. Their respective AE_{298} values, however, contradict these ideas. Therefore, the steric hindrance of molecular chlorine formation may also account for the raising of the AE_{298} for CHF^+ above that of CF^+. The CCl^+ ion may form with either HF + Cl or HCl + F as neutral fragments, with the former pair having a $\Delta_rH^0_{298,calc}$ value that is *ca.* 1.4 eV lower than the latter pair. We assign a mixture of both of these channels as responsible for CCl^+ production. The HF + Cl channel is also *ca.* 1 eV lower in energy than the $CHCl_2F^+ + h\nu \rightarrow CHCl^+ + ClF$ channel. This is consistent with the observed trend of AE_{298} data for these minor ions. A hydrogen atom is smaller than a chlorine atom, so fusion of a H–F bond is preferred to that of a Cl–F bond, and even provides some enthalpic compensation to overcome the breaking of a C–Cl bond. As before, this reaction appears to be driven by steric effects. The AE_{298} values for both of these minor ions do not occur at the thermochemical threshold. This can be credited to the energetically-accessible channels, which occur *via* a tight transition state with a large expected barrier to reaction as X = Cl.

The concurrence between the $\Delta_r H^0_{298,calc}$ values for $CHClF_2^+$ and CHF_2^+ formation from $CHClF_2$ and the $\Delta_r H^0_{298,exp}$ values shows that both ions are observed at their thermochemical thresholds. Breaking a C–F bond in the precursor ion yields a theoretical $\Delta_r H^0_{298,calc}$ value of 13.52 eV. This is significantly lower than $\Delta_r H^0_{298,exp}$ for $CHClF^+$ derived in this work. However, the ion yield profile for this fragment closely mimics that of the TPES and exists within the same span of energies, *ca.* 14–18 eV. This peak in the TPES is assigned as $\tilde{C}\ ^2A''/\tilde{D}\ ^2A''/\tilde{E}\ ^2A'$ states of the parent ion; therefore, we conclude that state-selected dissociation is occurring from these states. In order to be consistent with our experimental observations, CF_2^+ can only form with HCl as its partner neutral. The energetics of CF^+ production indicate that this ion is produced by the $CHClF_2^+ \rightarrow CF^+ + HF + Cl$ channel. This reaction has a lower threshold than the lowest CHF^+ channel, which forms with ClF. As this is analogous to the aforementioned $CCl^+/CHCl^+$ situation, we believe that steric effects make CF^+ formation energetically more favourable than production of CHF^+. X = F in these instances, so the comparatively moderate height of the barrier to reaction leads to a disparity between the calculated threshold and AE_{298}.

The $\Delta_r H^0_{298,calc}$ values for formation of the parent ion and C–Cl bond fission from CH_2ClF^+ compare well with our $\Delta_r H^0_{298,exp}$ values, therefore these ions form at their thermochemical thresholds. By contrast, CH_2Cl^+ production has a thermochemical limit of 13.38 eV, which is *ca.* 0.8 eV lower than the observed $\Delta_r H^0_{298,exp}$ for this ion. This value, however, is very close to the maximum of the $\tilde{B}$ state of the parent ion, so we assume that CH_2Cl^+ is produced by state-selective dissociation. The AE_{298} of CHF^+ is precisely the same as the lower calculated threshold of 13.38 eV, where HCl is the accompanying neutral fragment. This indicates that the reaction barrier height is negligible, as X = H. The CH_2^+ fragment is also observed at threshold, although any interpretation of these data should be accompanied by the caveat that there is an appreciable level of uncertainty in AE_{298} for this ion. Comparison of the $CHCl^+$ AE_{298} with thermochemistry predicts that the reaction where HF is produced as the neutral partner is the dominant channel. In the case of CCl^+ formation, however, two channels are energetically accessible, with either HF + H or H_2 + F as the accompanying species. This can be credited to the lack of steric bulk around the hydrogen atom, making H–H bond formation competitive. However, the amount of energy recovered *via* HF formation ensures that the former channel is still the most favourable. All three of the energetic channels to form CF^+ are open, with H_2 + Cl and HCl + H having practically the same $\Delta_r H^0_{298}$ value.

In summary, dissociation to form the major ion products displays the same trend in all three systems. The parent ion and first ionic product appear at the thermochemical onset, but the second ion fragment appears at an energy *ca.* 1 eV higher than the theoretical threshold. This trend has also been observed in the TPEPICO studies of the analogous parent ions $CH_2F_2^+$ and $CH_2Cl_2^+$.[33,36] In the present work, the first and second ions observed are formed *via* C–Cl and C–F bond fission, respectively. This holds true for the whole of this study, regardless of the parent molecule. The fact that a C–Cl bond is cleaved first is not surprising, as this is the weakest bond of the three available. For example, it is 68 and 116 kJ mol^{-1} less endothermic than C–H and C–F bond fission in $CHCl_2F$, respectively.[37] At higher energies, $CHCl_2F$ and $CHClF_2$ appear to behave in similar ways, in that fragmentation into smaller ions occurs in a comparable fashion, *e.g.* CF^+ is observed at lower photon energy than CHF^+. Although this result is counter-intuitive, our data is supported by thermochemical arguments and data obtained by other methods, as detailed in Sections 4.1.2 and 4.2.2. CH_2ClF appears to fragment in the more conventional manner, with sequential bond fission occurring as the photon energy is increased. However, it acts anomalously in the context of this study. This may be attributed to the small size of the hydrogen atom with respect to the sizes of the fluorine and chlorine atoms, and the inherent steric trend this implies.

5.2 Dissociation dynamics determination by analysis of $\langle KE \rangle_t$ and $\langle f \rangle_t$

Using the $\langle KE \rangle_t$ and $\langle f \rangle_t$ data listed in Table 3, we can infer the mechanism of dissociation for the single-bond-fission processes observed in these three molecules. The parent ion of $CHCl_2F$ is bound and non-dissociative in the ground and, possibly, first excited states. In the case of C–Cl bond cleavage from $CHCl_2F^+$, the $\langle f \rangle_t$ values for the $\tilde{X}\ ^2A''$ and $\tilde{A}\ ^2A'$ state fit the impulsive model. This observation can be rationalised by taking into account the nature of the molecular orbitals that are involved in ionization. As these states are formed by the removal of an electron from orbitals that are predominantly Cl lone pair in character,[10] a vacancy localised on a chlorine atom is created. This situation only exists for a very short time as the surrounding electron density redistributes rapidly to delocalise this charge, therefore at this energy this channel is only accessible by prompt dissociation.[19] Formation of both $CHClF^+$ and $CHCl_2^+$ occurs from dissociation of the near-degenerate $\tilde{D}\ ^2A''/\tilde{E}\ ^2A'$ states of the parent ion, indicating competition between C–Cl and C–F bond fission at this energy. The former bond undergoes a statistical dissociation, implying that there is a higher density of states at this higher energy than at the ground or first excited states, whereas the latter bond dissociates *via* an impulsive mechanism. As these spectra were recorded at 14.67 eV, which is nearer to the energy of the $\tilde{E}\ ^2A'$ state, it is expected that ionization at this energy is from an orbital that is essentially fluorine lone-pair in nature.[9] Therefore, a rapid dissociation would favour C–F bond cleavage. Conversely, a statistical dissociation should form a mixture of both ionic products. The C–Cl σ-bonding character of the $\tilde{D}\ ^2A''$ state [10] should not be ignored either, as the influence of this orbital at this intermediate photon energy would lead to preferential formation of $CHClF^+$. Our data appear to support these phenomena.

The lower vibrational levels of the ground state of $CHClF_2^+$ are bound. An impulsive mechanism for C–Cl bond dissociation is observed from the $\tilde{X}\ ^2A''/\tilde{A}\ ^2A'$ and $\tilde{B}\ ^2A'$ states of $CHClF_2^+$. These states are Cl lone pair and C–Cl σ-bonding in nature, respectively.[10] Therefore, dissociation from the ground and first excited states would occur *via* a vacancy on the chlorine atom, as described above, with dissociation from the $\tilde{B}\ ^2A'$ state clearly occurring by removal of a C–Cl bonding electron. Competition between statistical formation of CHF_2^+ and impulsive production of $CHClF^+$ from the unresolved $\tilde{C}\ ^2A''/\tilde{D}\ ^2A''/\tilde{E}\ ^2A'$ states can be explained by the nature of the electron removed from these orbitals. As all three states nominally arise due to removal of a fluorine lone-pair electron, this observation can be rationalised in the same way as the competition for C–F/C–Cl bond cleavage from $CHCl_2F^+$, also described above. We note that the behaviour for $CHCl_2F^+$ and $CHClF_2^+$ is analogous to that reported before for CCl_3F^+ and $CCl_2F_2^+$.[19,33]

In the case of CH_2ClF^+, the parent ion is bound over a larger energy range than that of the other two HCFCs. Photodissociation of CH_2ClF^+ at 14.03 and 14.32 eV leads predominantly to C–Cl bond cleavage. These energies relate to dissociation from the $\tilde{B}$ and $\tilde{C}$ states of the parent ion, and their $\langle f \rangle_t$ values fit the impulsive mechanism and a mixture of the two models, respectively. As the $\tilde{B}$ state is C–Cl σ-bonding in nature, removal of an electron results in fission of the C–Cl bond. However, the $\tilde{C}$ state has been assigned C–H σ-bond character,[8] so removal of an electron from this orbital should lead to removal of a hydrogen from the parent ion. As this is not observed, state-selected dissociation does not occur, and

 This journal is © The Owner Societies 2005

the $\langle f \rangle_t$ value suggests a combination of statistical and impulsive models. The competing processes resulting in CH_2F^+ and CH_2Cl^+ formation as a result of dissociation from the $\tilde{C}$ state appear to occur on different timescales, in accordance with the competing bond cleavage processes discussed previously. The $\langle f \rangle_t$ value for production of $CH_2Cl^+ + F$ at 17.44 eV shows that C–F bond fission from the $\tilde{E}/\tilde{F}$ states occurs *via* a mixture of the two models. As these two states exhibit fluorine lone pair and fluorine atom character,[8] the temporary vacancy mechanism described above may be possible. However, the dissociation process cannot proceed on the short timescale required for this mechanism to be viable, as the large density of states inferred by the high photon energy favours statistical pathways. Therefore, a hybrid mechanism is observed, consistent with our data.

6. Conclusions

By capitalising on the tunability of a synchrotron radiation source coupled to a VUV monochromator, and the ability of TPEPICO spectroscopy to excite state-selectivity of the parent ion, we have studied the photon-induced fragmentation of the valence states of $CHCl_2F^+$, $CHClF_2^+$ and CH_2ClF^+ between 11 and 25 eV. TPES, ion yield plots and breakdown diagrams[12] have been constructed, with the band shapes and positions of the former agreeing with previous He(I) and He(II) photoelectron spectra.[8,9] By comparison with thermochemistry, its has been demonstrated that all three HCFCs dissociate in a similar manner at low photon energy, with the parent and first fragment ions occurring at their thermochemical thresholds, but the second product ion is formed *ca.* 1 eV higher than its predicted threshold. This disparity indicates state-selected dissociation. However, at higher photon energies $CHCl_2F$ and $CHClF_2$ dissociate in an unexpected manner, with some ions formed by cleavage of three bonds possessing lower AE_{298} than some formed by cleavage of two bonds. CH_2ClF displays the more expected behaviour, *i.e.* stepwise cleavage with increasing photon energy. These observations can be rationalised in terms of the barrier size on the exit channel, as determined by the small steric bulk of the hydrogen atom compared to that of either a chlorine or fluorine atom. The mean kinetic energy releases have also been measured into the channels involving single bond cleavage of each of the HCFCs. These data allow the determination of the mechanism by which the decay proceeds. In common with previous work by this group, the fractional kinetic energy release for a single fragment decreases with increasing photon energy, indicating an apparent shift from impulsive to statistical behaviour. In some cases competition between statistical and impulsive processes is observed, for example C–Cl *vs.* C–F bond cleavage in $CHCl_2F^+$ and $CHClF_2^+$. Overall, this study has added to our knowledge of the VUV photochemistry of these three HCFC molecules, which may have atmospheric significance if these molecules are not removed rapidly by OH attack in the troposphere. The molecules also appear to display behaviour intermediate between the 'small' and 'large' molecule limits.[14]

Acknowledgements

We thank Dr Paul Hatherly (Reading University), Ian Sutton and Steve Davis (both of the CCLRC Daresbury Laboratory) for technical assistance. EPSRC is thanked for equipment grants and access to the Daresbury SRS (GR/M42794), and for studentships (CRH and DJC).

References

1 M. J. Molina and F. S. Rowland, *Nature*, 1974, **249**, 810.
2 R. P. Wayne, *Chemistry of Atmospheres*, 3rd edn., Oxford University Press, Oxford, 2000.
3 D. L. Hobrock and R. W. Kiser, *J. Phys. Chem.*, 1964, **68**, 575.
4 P. Cicman, K. Gluch, A. Pelc, W. Sailer, S. Matt-Leubner, P. Scheier, S. Matejcik, P. Lukac, W. D. Robertson, R. N. Compton and T. D. Mark, *J. Chem. Phys.*, 2003, **119**, 11704.
5 Y. W. Zhang, L. S. Sheng, F. Qi, H. Gao and S. Q. Yu, *J. Electron Spectrosc.*, 1996, **79**, 483.
6 F. C. Y. Wang and G. E. Leroi, *Ann. Isr. Phys. Soc.*, 1983, **6**, 210.
7 S. J. Pearton, W. S. Hobson, U. K. Chakrabarti, G. E. Derkits and A. P. Kinsella, *J. Vac. Sci. Technol. B*, 1990, **8**, 1274.
8 J. Doucet, P. Sauvageau and C. Sandorfy, *J. Chem. Phys.*, 1973, **58**, 3708.
9 I. Novak, T. Cvitas, L. Klasinc and H. Gusten, *J. Chem. Soc., Faraday Trans. 2*, 1981, **77**, 2049.
10 K. K. Irikura, M. A. Ali and Y. K. Kim, *Int. J. Mass Spectrom.*, 2003, **222**, 189.
11 X. H. Zhang, X. J. Chen, C. K. Xu, C. C. Jia, X. F. Yin, X. Shan, Z. Wei and K. Z. Xu, *Chem. Phys.*, 2004, **299**, 17.
12 C. R. Howle, C. A. Mayhew and R. P. Tuckett, *J. Phys. Chem. A*, 2005, **109**, 3626.
13 P. A. Hatherly, M. Stankiewicz, K. Codling, J. C. Creasey, H. M. Jones and R. P. Tuckett, *Meas. Sci. Technol.*, 1992, **3**, 891.
14 P. A. Hatherly, D. M. Smith and R. P. Tuckett, *Z. Phys. Chem. (Munich)*, 1996, **195**, 97.
15 D. M. P. Holland, J. B. West, A. A. MacDowell, I. H. Munro and A. G. Beckett, *Nucl. Instrum. Methods Phys. Res., Sect. B*, 1989, **44**, 233.
16 W. C. Wiley and I. H. MacLaren, *Rev. Sci. Instrum.*, 1955, **26**, 1150.
17 J. H. D. Eland, *Photoelectron Spectroscopy*, 2nd edn., Butterworths, London, 1984.
18 I. Powis, P. I. Mansell and C. J. Danby, *Int. J. Mass Spectrom. Ion Phys.*, 1979, **32**, 15.
19 D. P. Seccombe, R. Y. L. Chim, G. K. Jarvis and R. P. Tuckett, *Phys. Chem. Chem. Phys.*, 2000, **2**, 769.
20 G. K. Jarvis, D. P. Seccombe and R. P. Tuckett, *Chem. Phys. Lett.*, 1999, **315**, 287.
21 J. C. Traeger and R. G. McLoughlin, *J. Am. Chem. Soc.*, 1981, **103**, 3647.
22 M. W. Chase, *J. Phys. Chem. Ref. Data*, 1998, monograph no. 9.
23 J. L. Franklin, *Science*, 1976, **193**, 725.
24 K. E. Holdy, L. C. Klots and K. R. Wilson, *J. Chem. Phys.*, 1970, **52**, 4588.
25 G. E. Busch and K. R. Wilson, *J. Chem. Phys.*, 1972, **56**, 3626.
26 (*a*) W. Zhou, D. P. Seccombe, R. P. Tuckett and M. K. Thomas, *Chem. Phys.*, 2002, **283**, 419; (*b*) W. Zhou, D. J. Collins, R. Y. L. Chim, D. P. Seccombe and R. P. Tuckett, *Phys. Chem. Chem. Phys.*, 2004, **6**, 3081.
27 S. G. Lias, J. E. Bartmess, J. F. Liebman, J. L. Holmes, R. D. Levin and W. G. Mallard, *J. Phys. Chem. Ref. Data*, 1988, **17**, supplement no. 1.
28 B. Sztaray and T. Baer, *Rev. Sci. Instrum.*, 2003, **74**, 3763.
29 C. R. Brundle and A. D. Baker, *Electron Spectroscopy: Theory, Techniques and Applications*, Academic Press, New York, 1977, vol. 1.
30 For example, H. E. Stanton and J. E. Monaham, *J. Chem. Phys.*, 1964, **41**, 3694.
31 M. Seaver, J. W. Hudgens and J. J. Decorpo, *Int. J. Mass Spectrom. Ion Phys.*, 1980, **34**, 159.
32 NIST Chemistry Webbook, http://webbook.nist.gov/chemistry/.
33 D. P. Seccombe, R. P. Tuckett and B. O. Fisher, *J. Chem. Phys.*, 2001, **114**, 4074.
34 K. Takeshita, *Chem. Phys. Lett.*, 1990, **165**, 232.
35 J. L. Franklin, P. M. Hierl and D. A. Whan, *J. Chem. Phys.*, 1967, **47**, 3148.
36 R. Y. L. Chim, PhD Thesis, University of Birmingham, 2003.
37 E. Tschuikow-Roux and S. Paddison, *Int. J. Chem. Kinet.*, 1987, **19**, 15.